Inhibition of calcium carbonate and sulfate scales by a non-phosphorus terpolymer AA-APEY-AMPS

Yunyun Bu[a], Yuming Zhou[a,*], Qingzhao Yao[a,*], Yiyi Chen[a], Wei Sun[b], Wendao Wu[b]

[a]*School of Chemistry and Chemical Engineering, Southeast University, Nanjing 211189, P.R. China,*
emails: ymzhou@seu.edu.cn (Y. Zhou), 101006377@seu.edu.cn (Q. Yao)
[b]*Jianghai Environmental Protection Co., Ltd, Changzhou 213116, Jiangsu, P.R. China*

ABSTRACT

The inhibition of calcite crystal growth by acrylic acid-allylpolyethoxy carboxylate-2-acrylamido-2-methyl-propanesulfonic acid (AA-APEY-AMPS, PAYS for short) was investigated in the cooling-water system. The terpolymer was prepared via the copolymerization of acrylic acid (AA), allylpolyethoxy carboxylate (APEY) and 2-acrylamido-2-methyl-propanesulfonic acid (AMPS), whose structures were characterized by FTIR and ^{1}H NMR. In this study, we have investigated the effect of the agent concentration and the ratio of the reactant. The experimental results show that AA-APEY-AMPS is an effective chelating scale inhibitor and it has high efficiency toward scales and nearly 90% for calcium carbonate and 100% for calcium sulfate. The produced crystals were characterized by using scanning electron microscopy and X-ray diffraction methods. It appears that the crystal shape, size, and the morphology of scale have changed apparently at the dosage of 5 mg/L. Based on the contrast experiment of the problem of scale formation, this paper analyses the mechanism of scale formation and the advantage of PAYS. The supporting mechanism of scale formation was also described and analyzed briefly.

Keywords: Terpolymer; Non-phosphate antiscalant; Calcium carbonate; Calcium sulfate; Mechanism

1. Introduction

The most protruding question of cooling water systems is equipment corrosion and begriming. In the process of industrial water recovery in the cooling water technology, scales offer an obstruction to the heat flow when they crystallize on heat transfer surfaces and then the efficiency in heat transmission is greatly reduced, and the pipelines may become clogged with these sparingly soluble mineral salts [1–3]. Eventually, massive precipitation of insoluble salts accumulated to some extent facilitates the corrosion processes, and even causes catastrophic operational failures in some cases and then production has to be stopped occasionally [4,5]. The most common scales are calcium carbonate ($CaCO_3$), calcium sulfate ($CaSO_4$), barium sulfate ($BaSO_4$), calcium phosphate ($Ca_3(PO_4)_2$), calcium oxalate, silicate, etc. [6–9]. To control deposit formation and prevent the negative issues and deleterious effect evoked by scale precipitation, adding scale inhibitors to the circulating water system is the most common and effective way [10–13]. On the

*Corresponding authors.

whole, scale inhibitors added in industrial cooling water are more economical than free antiscalant because of high cost of removing deposition.

Considerable and effectual progress has been made in the development of practical processes and products application. In the past decades, scale inhibitors widely used in cooling water system are mainly poly (phosphate) and organophosphonate (such as HEDP (Hydroxy ethyly-dene-1,1-diphosphonate), EDTMP (ethylene-diamine-tetrakis(methylene-phosphonate)), and NTMP (nitrilo trimethylene phosphonate) [14–18]. However, the discharge of effluent that contains these sorts of scale inhibitors are likely to accelerate water eutrophication [19,20], and then to destroy the balance of ecological environment and cause water pollution even if they continue to be important for industry production, at present. Besides, phosphonates are supposed to form insoluble phosphonate scales when they reverted to orthophosphates and are also likely to serve potential nutrient to algae [21–23]. Thus, conventional phosphate-generating antiscalants are thought to be quite environmentally unfriendly. Increasing concerns and discharge limitations have changed the scale-inhibitor chemistry to green antiscalants that phosphate-free and nitrogen-free polymer for assistance. While there is a recent intense interest in improving the performance of carboxylic polymers for the inhibition of insoluble salt deposition, such as acrylic acid polymers (PAA) and maleic acid polymers (PMA) [24–27], these agents have significant properties which contain low dosage effect, definite solubility threshold effect, the synergetic effect with other reagents, and high temperature endurance. Unfortunately, they would not only react with calcium ions to form insoluble calcium-polymer salts due to their low calcium tolerance but also would limit the water solubility due to the strong intermolecular and intramolecular hydrogen bonds between the hydroxyl groups along the chain backbone [28,29].

A promising alternative for phosphonates is in the application of copolymer, which may be found—PAYS (poly(AA-APEY-AMPS)), whose structure contains many active groups such as carbonyl, allyloxy, amide, sulfonic acid, and ester had the advantage of chemical modification, such as simple experimental methods, low material costs, friendliness to environment and high inhibition capacity, especially, many antiscalants that based on the effect of sulfonic acid group and carbonyl group were reported in the literatures [30–32], for example, SO_3H groups in polymers can provide advantage for inhibition on $Ca_3(PO_4)_2$ [33,34], which lays the foundation for further research. And, then it may influence the polymorph selection, growth mechanism, nucleation, shape, structure and size of the

crystal. In this paper, we synthesized a new effective non-phosphorus scale inhibitor, and investigated its scale inhibition through the static scale-inhibiting method.

2. Experimental

2.1. Materials and instruments

The allylpolyethoxy carboxylate (APEY) used in the experiment was synthesized in our laboratory according to K. Du's procedure. Both acrylic acid (AA), maleic anhydride (MA), $CaCl_2$, $NaHCO_3$, Na_2SO_4, ethylenediaminetetraacetic acid disodium salt (EDTA·2Na), and ammonium persulfate were analytically pure grade and supplied by Zhongdong Chemical Reagent Co., Ltd (Nanjing, China). The commercial inhibitors of PAA (MW = 1,800), HPMA (MW = 600), PESA (MW = 1,500), HEDP (MW = 206), APEG (MW = 300), and 2-acrylamido-2-methyl-propanesulfonic acid (AMPS) were technical grade and were supplied by Jiangsu Jianghai Chemical Co., Ltd. Deionized water was used throughout the experiments.

The FTIR spectra were recorded for the synthesized polymer to confirm the functional groups that are responsible for the antiscaling property using a Bruker FTIR analyzer (VECTOR-22, Bruker Co., Germany) in the pressed KBr pellets. ^{1}H NMR spectra were taken by a Mercury VX-500 spectrometer (Bruker AMX500) with a tetramethylsilane internal reference and deuterated dimethyl sulfoxide as the solvent. The shapes of $CaCO_3$ and $CaSO_4$ were observed with scanning electron microscopy (SEM; S-3400 N, HITECH, Japan). The X-ray diffraction (XRD) studies were carried out using a Rigaku D/max 2400 X-ray powder diffractometer with Cu Kα radiation ($\lambda = 1.5406$, 40 kV, 120 mA).

2.2. Synthesis of antiscalant

The synthesis procedure of APEY is shown in Scheme 1. It was synthesized from allyloxy polyethoxy ether (APEG) and MA at room temperature. A new additive (acrylic acid-allylpolyethoxy carboxylate-2-acrylamido-2-methyl-propanesulfonic acid, PAYS) was prepared as following (Scheme 2) and the modified conditions were based on our preparative experiments. In brief, a 4-neck round bottom flask, equipped with a thermometer and a magnetic stirrer, was filled with 5 mL of deionized water and 2 g APEY and then heated to 70°C with stirring under nitrogen atmosphere. After that, 4 g AA and 1 g 2-acrylamido-2-methyl-propanesulfonic acid (AMPS) was added in 20 mL distilled water and the initiator solution (0.21 g

ammonium persulfate in 20 mL distilled water) was injected into the flask separately at constant flow rates over a period of 1.0 h. After that, the flask was then heated to 80°C for 1.5–2.5 h with stirring to finally obtain the faint yellow liquid with an approximately 25% solid content.

2.3. Static scale inhibition methods

All inhibitor dosages given below were on a dry-inhibitor basis. In this experiment, the effectiveness of PAYS against calcium carbonate precipitation was determined according to the national standard of P.R. China concerning the code for the design of industrial circulating cooling-water treatment (GB/T 16632-2008) by the static scale inhibition test under different conditions, taking $CaCl_2$ and $NaHCO_3$ solutions. The final concentration of Ca^{2+} and HCO_3^- was 240 and 732 mg L^{-1}, respectively, with the solution pH 9 adjusting by borax buffer solution. Investigations with inhibitors and without inhibitors were all carried out. To avoid the concentration of the solution by evaporation especially at a high temperature, we condensed the vapor by means of a cooler. Deposition of these calcium carbonate supersaturated solutions was filtered using filter paper after these solutions were incubated at 80°C for 10 h in water bath. During the experiment, the solution temperature and the flow velocity were all kept constant. Then, they were cooled (about 4–5 h) to ambient temperature. The remaining Ca^{2+} ions concentration in the supernatant was titrated by EDTA standard solution according to the national standard of P.R. China concerning the code for the design of industrial circulating cooling water treatment (GB/T 15452-2009). At the end point of titration, the color of the solution changed from purple red into dark blue using calcon carboxylic acid indicator. The copolymer inhibition efficiency of PAYS against calcium carbonate scale was calculated as Eq. (1) [2]:

$$\text{Inhibition efficiency } \eta \ (\%) = \frac{C_1 - C_0}{C_2 - C_0} \tag{1}$$

where C_2 (mg/L) was an original Ca^{2+} concentration before the test, C_0 was a final Ca^{2+} concentration in the absence of scale inhibitor PAYS, and C_1 was a final Ca^{2+} concentration in the presence of scale inhibitor PAYS.

The procedure of calcium sulfate inhibition test was alike to calcium carbonate experiments according to the national standard of P.R. China concerning the code for the design of industrial oilfield-water treatment (SY/T 5673-93). Calcium sulfate precipitation

and inhibition were studied in artificial cooling water which was prepared by dissolving a certain quantity of $CaCl_2$ and Na_2SO_4 in deionized water. Two concentrations of $CaCl_2$ (6,800 mg/L Ca^{2+}) and Na_2SO_4 (7,100 mg/L SO_4^{2-}). The pH of the calcium sulfate solutions were adjusted to 7.0 using hydrochloric acid or sodium hydroxide. The artificial cooling water containing different quantities of the PAYS copolymer was thermo-stated at 60°C for 10 h in water bath, the determination of Ca^{2+} was exactly the same as processed. The inhibition efficiency of PAYS against calcium sulfate scale was calculated as Eq. (1).

3. Results and discussion

3.1. Characterization of inhibitor

The FTIR spectra was taken for APEG, APEY, and the synthesized PAYS are depicted in Fig. 1. Functional groups were assigned for the characteristic peaks, a broad band at 3,440 cm^{-1} corresponds to O–H stretching vibrations of hydroxyl group. The strong intensity absorption peak that appear at 1,728 cm^{-1} (–C=O) in curve b indicates that APEY has been synthesized successfully when compared with curve (a). The band at 1,643 cm^{-1} could be C=O stretching vibrations that appears in curve (a) and (b) but disappears almost completely in curve (c), the residuary weak peak could be C=O of amid group or the incomplete reaction. Band at 1,543 cm^{-1} reveal C–N stretching vibrations and N–H flexural vibrations. The peak at 1,458 cm^{-1} is due to the –CH_2 scissoring deformation vibration. The peaks that appear at 1,039 and 1,171 cm^{-1} are assigned for aliphatic –S=O symmetry and asymmetry stretching vibrations of sulfonic acid
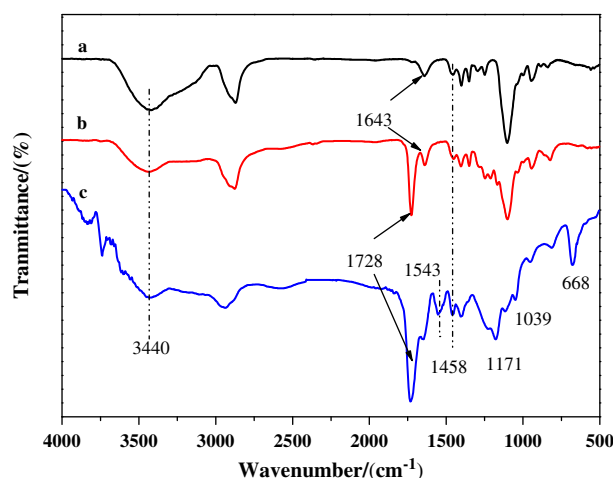
Fig. 1. FTIR spectrum of APEG (a), APEY (b), and PAYS (c).

groups, respectively, and the S–O stretching peaks at 668 cm^{-1} [29,35]. The expected functional groups, which are responsible for the inhibiting character of the PAYS, are confirmed basically.

The ^{1}H NMR spectra of APEG, APEY, AMPS, and PAYS are presented in Fig. 2. The ^{1}H NMR data were acquired as the following and the chemical molecule structures were deduced as expected.

APEG(a) ((CD$_3$)$_2$SO, δ ppm): 2.50 (solvent residual peak of (CD$_3$)$_2$SO), 3.29–3.53 (–OCH$_2$CH$_2$–, ether group), 3.94 (CH$_2$=CH–CH$_2$–, propenyl protons), 4.51–4.54 (–OH, active hydrogen in APEG), 5.12–5.92 (CH$_2$=CH–CH$_2$–, propenyl protons).

APEY(b) ((CD$_3$)$_2$SO, δ ppm): 2.50 (solvent residual peak of (CD$_3$)$_2$SO), 3.49–3.84 (–OCH$_2$CH$_2$–, ether group), 3.94 (CH$_2$=CH–CH$_2$–, propenyl protons), 4.2 (–CH=CH–, ethylene protons), 5.12–5.91 (CH$_2$=CH–CH$_2$–, propenyl protons), 6.25–6.41 (–CH=CH–, ethylene protons).

AMPS(c) ((CD$_3$)$_2$SO, δ ppm): 2.50 (solvent residual peak of (CD$_3$)$_2$SO), 1.24–1.43 (–CH$_3$, methyl proton), 2.73 (–CONH–, acylamino), 4.74 (–CH$_2$–, methylene protons), 5.49–6.07 (CH$_2$=CH–, ethylene protons).

PAYS(d) ((CD$_3$)$_2$SO, δ ppm): 2.50 (solvent residual peak of (CD$_3$)$_2$SO), 1.23–1.75 (–CH$_3$, methyl proton), 2.20 (–CONH–, acylamino), 3.42 (–OCH$_2$CH$_2$–, ether group), 4.15 (–CH$_2$–, methylene protons).

The disappeared peak at 4.51–4.54 ppm (–OH) and appeared peak at 4.2, 6.25–6.41 ppm (–CH=CH–) in Fig. 2(b) demonstrates that active hydroxyl group in APEG has reacted with MA. Meanwhile, it was obvious that the double bond absorption peaks (δ = 5.12–5.91, 5.49–6.07, 4.2, and 6.25–6.41 ppm) disappeared completely in Fig. 2(d) when compared to Fig. 2(b) and (c), all of these data have been able to suggest that PAYS was synthesized successfully.

It can conclude from FTIR and ^{1}H NMR analysis that the presence of anticipated structure has been identified.

3.2. Effect of inhibitor on calcium scales

Scale inhibitor concentration and mole ratio greatly influence the performance of antiscalant PAYS. Tables 1 and 2 show the relationship between the inhibitor dosage and the inhibition capacity toward the CaCO$_3$ and CaSO$_4$ scales. As can be seen, the scale inhibition efficiency increased with the increasing concentration of the trimer, and their protection effect increased. It was obvious that when the dosage was 10 ppm (=10 mg/L), PAYS had a maximum calcium tolerance, with 85% CaCO$_3$ inhibition efficiencies while the performance has declined more or less as further increasing concentration, from Fig. 3. As

shown in Fig. 4, the maximum inhibition efficiency reached 100% when the dosage was only 7 ppm less than the dosage of the great majority of inhibitor on the market for CaSO$_4$. However, higher range PAYS, increasing trend of the inhibition efficiency was weakening or even decreased growth alike for CaCO$_3$. The copolymer molecular chain contains carboxylate (–COOH), carboxamide (–CONH), and sulfonate (–SO$_3$H) groups which have positive dispersion, excellent chelation, superior compatibilization with Ca^{2+} ion and lattice distortion ability. It is those active functional groups that possess good properties for Ca scale. For the same scale inhibitor, as the concentration gradually increased, the interaction between the scale inhibitor and Ca^{2+} ion became increasingly stronger, and the scale inhibitive performance of the polymer also improved. When scale inhibitor PAYS at the dosage of 10 ppm and 3 ppm, the inhibition efficiency reached 85% and 95% for CaCO$_3$ and CaSO$_4$, respectively. However, with excessive amount of multipolymer, the flocculation phenomenon was created because of strong polar interaction of active groups on the molecular chain, leading to the performance of antisalant PAYS, which decreased slightly for CaCO$_3$ and CaSO$_4$. With the same concentration of PAYS, the CaCO$_3$ scale inhibition efficiency value was observed to decrease in the order: 2:0.3:0.5 (AA:APEY:AMPS, mole ratio) > 2:0.5:0.5 > 2:1:0.5 > 2:1.5:0.5 > 2:1:1.5 > 2:1:1, whereas Tab.2 manifests that PAYS (AA:APEY:AMPS = 2:1:0.5, mole ratio) show superior efficiency in calcium sulfate inhibition than other mole ratio.

3.3. Comparisons of inhibition efficiency

The ability of AA-APEY-AMPS (2:0.3:0.5 and 2:1:0.5) to control calcium deposits was compared with HEDP(1-hydroxyethylidine 1,1-diphos-phonic acid), PESA (poly(epoxysuccinic acid), PAA (poly(acrylic acid)), and HPMA (hydrolytic poly(maleic anhydride)), which are low-phosphorus and phosphorus polymers. As can be seen in Fig. 3, the order of the capability power on CaCO$_3$ is as follows: PAYS > HEDP > PESA > HPMA > PAA, it is worth mentioning that the threshold dosage is 10 mg/L for PAYS as CaCO$_3$ antiscalant and anti-scaling rate reached the highest which was 89.2%, however, HEDP has an advantage in the threshold dosage (only 4 mg/L), but at which HEDP has only 63% calcium carbonate inhibition. As shown in Fig. 4, it was indicated that the order of preventing the precipitation of CaSO$_4$ was PAYS > PAA > HEDP > PESA > HPMA, the ultimate inhibition efficiency values were 100, 95.2, 93.6, 93.6, and 89.6%, respectively, which is in accordance with the results of assumption.
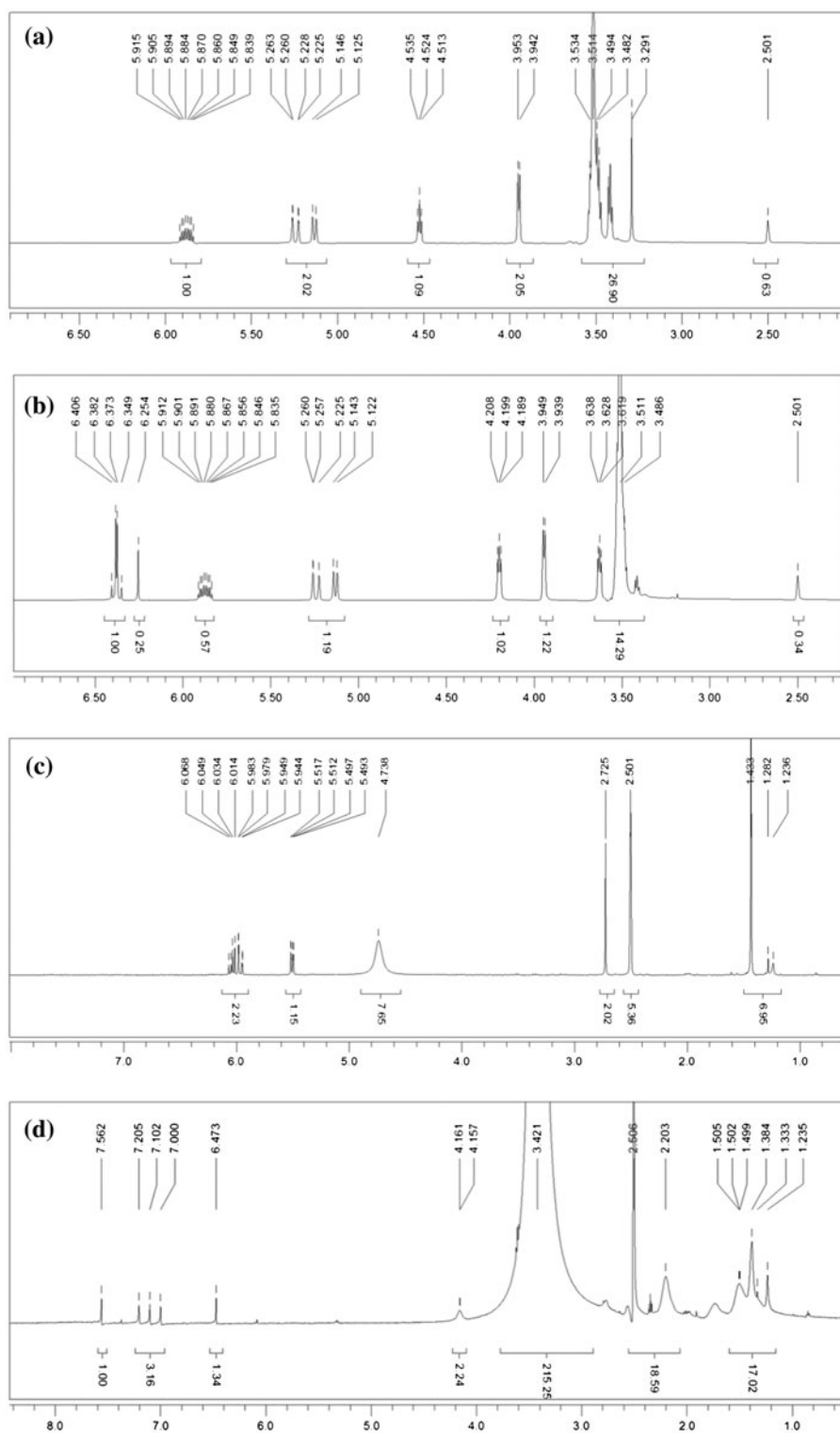
Fig. 2. ¹H NMR spectra of (a) APEG, (b) APEY, (c) AMPS, and (d) PAYS.

Table 1
Influence of the dosage and mole ratio of PAYS on the inhibition tests of $CaCO_3$

Dosage of inhibitor (ppm)	2:1:1.5 (%)	2:1:1 (%)	2:1:0.5 (%)	2:1.5:0.5 (%)	2:0.5:0.5 (%)	2:0.3:0.5 (%)
2	37.7	36.6	47.8	44.3	32.0	43.4
4	42.2	42.4	48.9	51.6	47.4	57.3
6	44.8	45.5	57.3	54.4	52.9	65.1
8	53.4	57.8	65.7	58.7	57.6	77.4
10	55.7	60.4	72.3	63.5	63.9	84.5
12	61.2	64.1	78.4	68.8	69.2	87.6
14	67.7	69.8	82.3	75.3	74.7	89.2
16	65.8	66.3	80.6	73.2	78.9	86.1

Table 2
Influence of the dosage and mole ratio of PAYS on the inhibition tests of $CaSO_4$

Dosage of inhibitor (ppm)	2:1:1.5 (%)	2:1:1 (%)	2:1:0.5 (%)	2:1.5:0.5 (%)	2:0.5:0.5 (%)	2:0.3:0.5 (%)
1	62.3	77.6	85.3	41.5	50.8	54.0
3	90.4	93.2	95.9	85.2	95.7	88.4
5	97.3	98.6	99.3	99.8	100	95.4
7	100	100	100	100	100	100
9	98.6	100	97.8	98.7	97.3	97.3
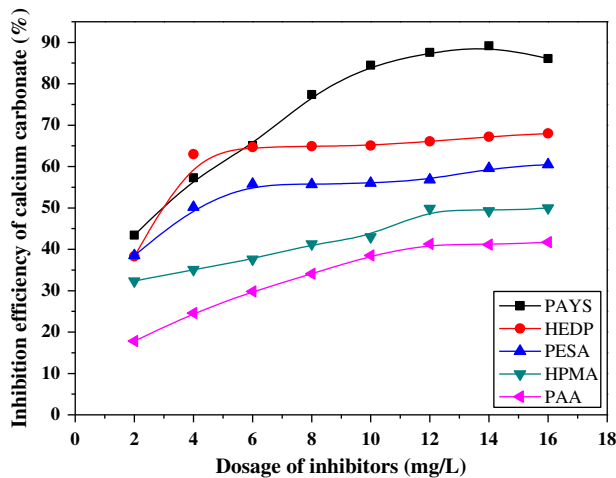
Fig. 3. Comparison of inhibition efficiency for $CaCO_3$ on calcium carbonate.
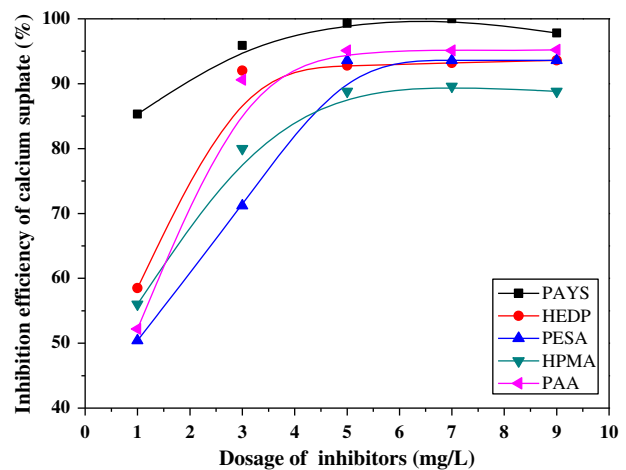
Fig. 4. Comparison of inhibition efficiency for $CaSO_4$ on calcium sulfate.

3.4. Characterization of scales

3.4.1. SEM studies

The SEM micrographs of $CaCO_3$ precipitate formed in simulative cooling water are shown in Fig. 5. The SEM image revealed the formation of well-regulated cubic octahedral crystal shaped [3,9] particles with average particle size about 10 μm in the absence of PAYS polymer (Fig. 5(a)). However, on addition of 2 ppm of the additive, the SEM micrographs of particles are shown in Fig. 5(b), it has obvious changes at the distribution and size. The grown crystals were smaller in size about 5 μm and the shape edges disappeared, a cluster of grain-shaped particles. It appeared that, in the presence of 6 ppm PAYS, the morphology has been modified to flaky or lamella shape (Fig. 5(c)),
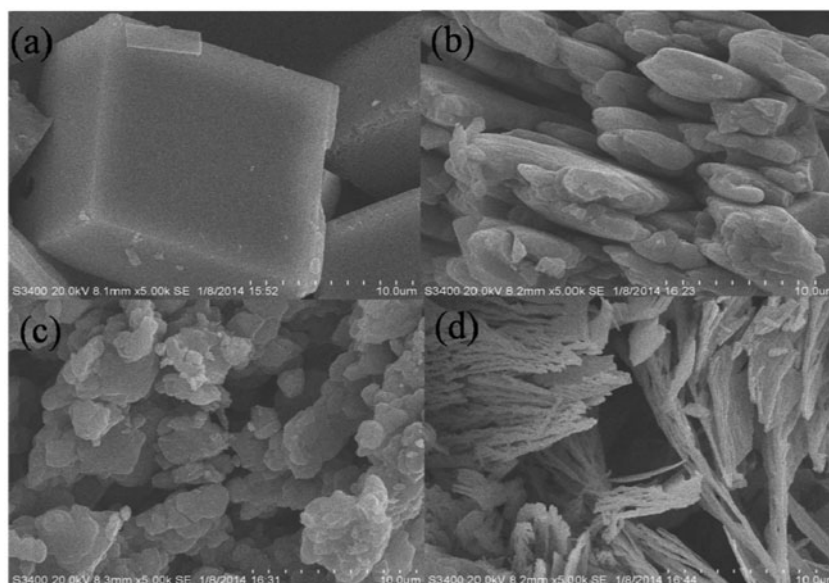
Fig. 5. SEM photographs for the calcium carbonate: (a) with the presence of PAYS, (b) 2 ppm, (c) 6 ppm, and (d) 10 ppm.
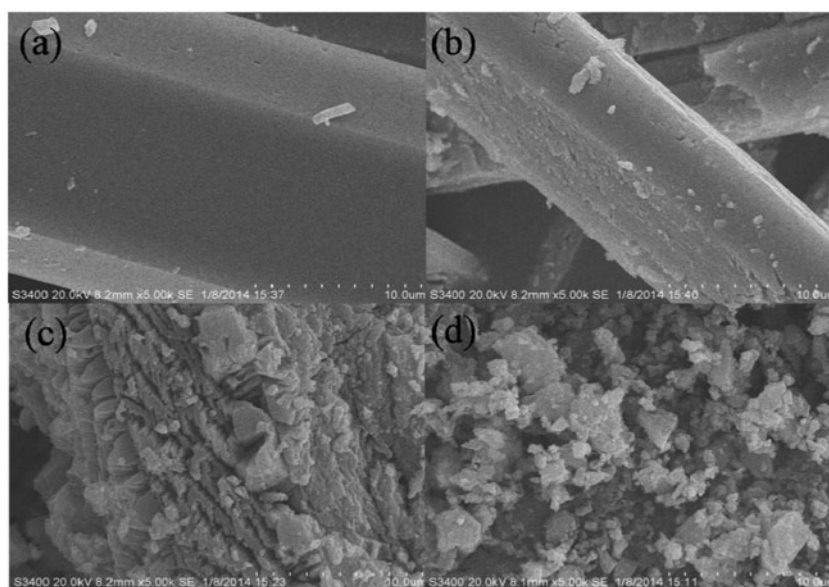
Fig. 6. SEM photographs for the calcium sulfate: (a) with the presence of PAYS, (b) 1 ppm, (c) 3 ppm, and (d) 5 ppm.

and silk-like shaped with hollow crystals (Fig. 5(d)) were obtained at the dosage of 10 ppm. The higher the concentration of PAYS was, the greater the change was, and the precipitates were amorphous, porous, and irregular. All of these changes indicate that the terpolymer affects the nucleation and morphology of the CaCO$_3$ precipitate, and the influence strengthened with increasing concentration of the PAYS.

The SEM pictures for calcium sulfate scale with the absence and the presence of the polymer PAYS are presented in Fig. 8. In the absence of the PAYS, the precipitates which were deposited had the form as shown in Fig. 6(a). As can be seen, calcium sulfate crystals are regular thin tubular cells and rod-shaped exhibiting monoclinic symmetry [9]. In the presence of 1 ppm PAYS, the crystal have roughened faces and appeared mass cracks (Fig. 6(b)), and the loose and rugged CaSO$_4$ precipitates was obtained (Fig. 6(c)). With the continued increase in the additive dosage, the crystal was destroyed and crumbled entirely (Fig. 6(d))

at level of 5 ppm. After the inhibition period, sharp edges and corners of the crystals disappeared almost completely, the sharp edges and crystallinity were changed, and the morphology of $CaSO_4$ was modified, whereas spongy deposits were formed and could be easily washed away by running water.

3.4.2. XRD studies

The XRD results for the carbonate and sulfate crystals of calcium with and without the presence of the polymer are presented in Figs. 7(a, b) and 8(a, b), respectively. As we all know, $CaCO_3$ exists in three types of crystal forms: calcite, aragonite, and vaterite. Untreated $CaCO_3$ crystallizes as prismatic calcite, which is the most thermodynamically stable crystal in Fig. 7(a), and the diffraction peaks appear at 012, 104, 006, 110, 113, 202, 018, and 116. The peaks of the precipitates with 4 ppm PAYS added, appear at 110, 112, 114, and 300 corresponding to vaterite (the least thermodynamically stable), with the exception of calcite peaks [3]. These results showed that, for a calcium carbonate, both calcite and vaterite formed, revealed that calcium carbonate would first nucleate and precipitate as calcite and then transited to a more unstable phase (vaterite) after 4 ppm PAYS was added [3]. These results are consistent with the SEM results, confirming the effect of PAYS. However, in the case of calcium sulfate, the interplanar crystal spacing (d) and angle of intersection (θ) values conformed to the
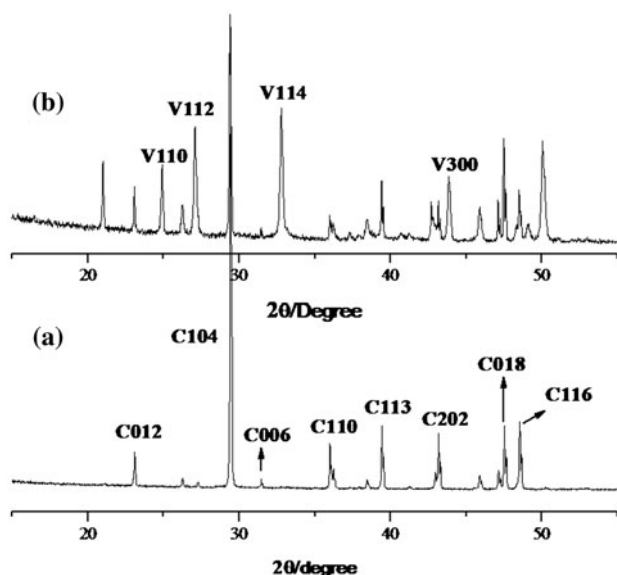
Fig. 8. XRD spectrum of $CaSO_4$ precipitates: (a) in the absence of an inhibitor and (b) in the presence of 3 ppm PAYS, respectively.

structure of gypsum ($CaSO_4·2H_2O$, calcium sulfate dihydrate) [9], there is no modification in their d and θ values from Fig. 8, the addition of polymers did not modify the crystal structure which would be confirmed but there were changes in the morphology, as is evident from the SEM photographs.

3.5. The mechanism of calcium scale inhibition

The above results indicated that when using the PAYS additives during the crystallization, the structure of calcium scales and crystal morphology were modified. This modification was due to the alteration of the crystal formation process, generation of crystal nucleus, and crystal nucleus growth [36]. It was most likely attributed to the carboxylic acid groups bind multivalent cation with powerful affinities and possess excellent chelate ability. First of all, PAYS could form soluble complexes with Ca^{2+} through –COOH, and the sulfonic acid groups enhanced polymer solubility and then make the molecular chain extension better, thereupon, the molecular chain encapsulates Ca^{2+} or crystal nucleus more easily [29]. The specified function and dispersion result from spatial repulsion was strengthened in water solution because of the strong hydrogen bonding between the water molecules and the –COOR groups. The polymer PAYS contained many –COO– groups in its molecules although the low concentration and the PAYS–Ca complexes could weaken the free Ca^{2+} activity and reduce the degree of supersaturation, so that the generation of crystal nucleus

Fig. 7. XRD spectrum of $CaCO_3$ precipitates: (a) in the absence of an inhibitor and (b) in the presence of 4 ppm PAYS, respectively.

$$CH_2=CHCH_2-O+(CH_2CH_2O)_{10}H \quad + \quad O=CHC=CHC=O$$

$$\xrightarrow{20\,°C} \quad CH_2=CHCH_2-O+(CH_2CH_2O)_{10}CCH=CHCOOH$$

Scheme 1. Synthesis of APEY.

$$CH_2=CHCH_2-O+(CH_2CH_2O)_{10}CCH=CHCOOH \quad + \quad CH_2=CHCOOH$$

$$+ \quad H_2C=C-C-NH-C-CH_2SO_3H$$

$$\xrightarrow[80\,°C]{2h}$$

Scheme 2. Synthesis of AA/APEY/AMPS (PAYS).

processing was almost ruined. The higher the chelate capability, stronger specific interaction with the inhibitor increased below the threshold, more effective the PAYS is. Otherwise, the inhibitor can tightly adsorb onto calcium crystalline substrate owing to –COO– of APEY segment and –SO$_3$H interaction with electric charge in the surface of crystal nucleus, the growth inhibition is caused by polymer adsorption of the active growth sites on crystal surfaces, and then inhibiting the growth of the crystal of calcium scale [3,37–39]. It is the strong interaction between the terpolymer and calcium carbonate and the adsorption that disturb the formation of typical calcium scale rhombohedra. It can be inferred that the terpolymer presumably adsorbing and chelating the scale nucleus, and thus prevents further growth.

4. Conclusion

The terpolymer PAYS was synthesized successfully by APEY (prepared in our laboratory before), AA, and 2-acrylamido-2-methyl-propanesulfonic acid, and the structure was characterized by FTIR and ^{1}H NMR. The performance of CaCO$_3$ and CaSO$_4$ scale were investigated by static scale inhibition method. The results of the present study are summarized as follows:

(1) The percentage inhibition efficiency of PAYS was observed to decrease in the following order: 2:0.3:0.5 (AA:APEY:AMPS, mole ratio) > 2:0.5:0.5 > 2:1:0.5 > 2:1.5:0.5 > 2:1:1.5 > 2:1:1, and exhibited 85% inhibition efficiency at the dosage of 10 ppm.

(2) PAYS is an effective CaSO$_4$ inhibitor under condition of pH 7, and about 5 ppm combination of PAYS provides almost 100% inhibition efficiency.

Characterization of CaCO$_3$ and CaSO$_4$ scales was examined by scanning electron microscopy, the SEM micrographs revealed that obvious change at the distribution, size, and morphology of scales occurred under the effect of PAYS. The XRD study also showed that the PAYS did not alter the crystallinity or the crystal structure but changed the morphology and size of the scales. These results indicate that PAYS is a potentially effective green alternative in inhibiting scales for circulating cooling water.

References

[1] H. Zhang, F. Wang, X. Jin, A botanical polysaccharide extracted from abandoned corn stalks: Modification and evaluation of its scale inhibition and dispersion performance, Desalination 326 (2013) 55–61.

[2] C.E. Fu, Y.M. Zhou, G.Q. Liu, J.Y. Huang, W. Sun, W.D. Wu, Inhibition of $Ca_3(PO_4)_2$, $CaCO_3$, and $CaSO_4$ precipitation for industrial recycling water, Ind. Eng. Chem. Res. 50 (2011) 10393–10399.

[3] C. Wang, S.P. Li, T.D. Li, Calcium carbonate inhibition by a phosphonate-terminated poly(maleic-co-sulfonate) polymeric inhibitor, Desalination 249 (2009) 1–4.

[4] E. Barouda, K.D. Demadis, S.R. Freeman, F. Jones, M.I. Ogden, Barium sulfate crystallization in the presence of variable chain length amino methylene tetra phosphonates and cations (Na^+ or Zn^{2+}), Cryst. Growth Des. 7 (2007) 321–327.

[5] F.M. Mahgoub, B.A. Abdel-Nabey, Y.A. El-Samadisy, Adopting a multipurpose inhibitor to control corrosion of ferrous alloys in cooling water systems, Mater. Chem. Phys. 120 (2010) 104–108.

[6] P. Shakkthivel, T. Vasudevan, Newly developed itaconic acid copolymers for gypsum and calcium carbonate scale control, J. Appl. Polym. Sci. 103 (2007) 3206–3213.

[7] A.L. Kavitha, T. Vasudevan, H.G. Prabu, Evaluation of synthesized antiscalants for cooling water system application, Desalination 268 (2011) 38–45.

[8] G. Jing, X. Li, Dynamic laboratory research on synergistic scale inhibition effect of composite scale inhibitor and efficient electromagnetic anti-scaling instrument, Res. J. Appl. Sci. Eng. Technol. 18 (2013) 3372–3377.

[9] P. Shakkthivel, T. Vasudevan, Acrylic acid-diphenylamine sulphonic acid copolymer threshold inhibitor for sulphate and carbonate scales in cooling water systems, Desalination 197 (2006) 179–189.

[10] H. Brinis, M.E.H. Samar, A method of making an aqueous dispersion of polyaniline and inhibiting corrosion in cooling water, Desalin. Water Treat. 44 (2012) 190–196.

[11] Suharso, Buhani, S. Bahri, T. Endaryanto, Gambier extracts as an inhibitor of calcium carbonate ($CaCO_3$) scale formation, Desalination 265 (2011) 102–106.

[12] T. Kumar, S. Vishwanatham, S.S. Kundu, A laboratory study on pteroyl-L-glutamic acid as a scale prevention inhibitor of calcium carbonate in aqueous solution of synthetic produced water, J. Pet. Sci. Eng. 71 (2010) 1–7.

[13] W.N. Al-Nasser, F.H. Al-Salhi, M.J. Hounslow, A.D. Salman, Inline monitoring the effect of chemical inhibitor on the calcium carbonate precipitation and agglomeration, Chem. Eng. Res. Des. 89 (2011) 500–511.

[14] K.D. Demadis, A. Ketsetzi, Degradation of phosphonate-based scale inhibitor additives in the presence of oxidizing biocides: "Collateral Damages" in industrial water systems, Sep. Sci. Technol. 42 (2007) 1639–1649.

[15] J. Marín-Cruz, R. Cabrera-Sierra, M.A. Pech-Canul, I. González, EIS characterization of the evolution of calcium carbonate scaling in cooling systems in presence of inhibitors, J. Solid State Electrochem. 11 (2007) 1245–1252.

[16] M. Pijuan, L. Ye, Z. Yuan, Free nitrous acid inhibition on the aerobic metabolism of poly-phosphate accumulating organisms, Water Res. 44 (2010) 6063–6072.

[17] J. Guo, S.J. Severtson, Inhibition of calcium carbonate nucleation with aminophosphonates at high temperature, pH and ionic strength, Ind. Eng. Chem. Res. 43 (2004) 5411–5417.

[18] S.J. Dyer, C.E. Anderson, G.M. Graham, Thermal stability of amine methyl phosphonate scale inhibitors, J. Pet. Sci. Eng. 43 (2004) 259–270.

[19] Z. Amjad, Investigations on the evaluation of polymeric calcium sulfate dihydrate (gypsum) scale inhibitors in the presence of phosphonates, Desalin. Water Treat. 37(1–3) (2012) 268–276.

[20] L. Boels, G.J. Witkamp, Carboxymethyl inulin biopolymers: A green alternative for phosphonate calcium carbonate growth inhibitors, Cryst. Growth Des. 11 (2011) 4155–4165.

[21] K. Chauhan, R. Kumar, M. Kumar, P. Sharma, G.S. Chauhan, Modified pectin-based polymers as green antiscalants for calcium sulfate scale inhibition, Desalination 305 (2012) 31–37.

[22] M.M. Nederlof, J. van Paassen, R. Jong, Nanofiltration concentrate disposal: Experiences in The Netherlands, Desalination 178 (2005) 303–312.

[23] A.A. Koelmans, H.A. Vander, L.M. Knijff, Integrated modelling of eutrophication and organic contaminant fate & effects in aquatic ecosystems, Water Res. 35 (2001) 3517–3536.

[24] A.D. Wallace, A. Al-Hamzah, C.P. East, W.O. Doherty, C.M. Fellows, Effect of poly(acrylic acid) end-group functionality on inhibition of calcium oxalate crystal growth, J. Appl. Polym. Sci. 116 (2010) 1165–1171.

[25] A.L. Kavitha, T. Vasudevan, H.G. Prabu, Evaluation of synthesized antiscalants for cooling water system application, Desalination 268 (2011) 38–45.

[26] D.W. Andrew, A.H. Ali, P.E. Christopher, O.S.D. William, M.F. Christopher, Effect of poly(acrylic acid) end-group functionality on inhibition of calcium oxalate crystal growth, J. Appl. Polym. Sci. 116 (2010) 1165–1171.

[27] P. Shakkthivel, T. Vasudevan, Newly developed itaconic acid copolymers for gypsum and calcium carbonate scale control, J. Appl. Polym. Sci. 103 (2007) 3206–3213.

[28] C. Wang, D.Y. Zhu, X.K. Wang, Low-phosphorus maleic acid and sodium p-styrenesulfonate copolymer as calcium carbonate scale inhibitor, J. Appl. Polym. Sci. 115(4) (2010) 2149–2155.

[29] Y. Bao, J. Ma, N. Li, Synthesis and swelling behaviors of sodium carboxymethyl cellulose-g-poly(AA-co-AM-co-AMPS)/MMT superabsorbent hydrogel, Carbohydr. Polym. 84 (2011) 76–82.

[30] A. Sand, M. Yadav, K. Behari, Preparation and characterization of modified sodium carboxymethyl cellulose via free radical graft copolymerization of vinyl sulfonic acid in aqueous media, Carbohydr. Polym. 81 (2010) 97–103.

[31] Z.M. Wang, L. Li, K.J. Xiao, J.Y. Wu, Homogeneous sulfation of bagasse cellulose in an ionic liquid and anticoagulation activity, Bioresour. Technol. 100 (2009) 1687–1690.

[32] Z. Reddad, C. Gérente, Y. Andrès, J.F. Thibault, P. Le Cloirec, Cadmium and lead adsorption by a natural polysaccharide in MF membrane reactor: Experimental analysis and modelling, Water Res. 37 (2003) 3983–3991.

[33] L.J. Gao, J.Y. Feng, B. Jin, Q.N. Zhang, T.Q. Liu, Y.Q. Lun, Z.J. Wu, Carbazole and hydroxy groups-tagged Poly(aspartic acid) scale inhibitor for cooling water systems, Chem. Lett. 40 (2011) 1392–1394.

[34] F. Karadeniz, M.Z. Karagozlu, S.-Y. Pyun, S.-K. Kim, Sulfation of chitosan oligomers enhances their anti-adipogenic effect in 3T3-L1 adipocytes, Carbohydr. Polym. 86 (2011) 666–671.

[35] S.B. Lin, C.H. Yuan, A.R. Ke, Z.L. Quan, Electrical response characterization of PVA–P(AA/AMPS) IPN hydrogels in aqueous Na_2SO_4 solution, Sens. Actuators, B 134(1) (2008) 281–286.

[36] G.Q. Liu, J.Y. Huang, Y.M. Zhou, Q.Z. Yao, L. Ling, P.X. Zhang, C.E. Fu, W.D. Wu, W. Sun, Acrylic acid-allyl-polyethoxy carboxylate copolymer dispersant for calcium carbonate and iron(III) hydroxide scales in cooling water systems, Tenside Surfact. Det. 49 (2012) 216–224.

[37] K.D. Demadis, S.D. Katarachia, Metal-phosphonate chemistry: Synthesis, crystal structure of calcium-amino tris-(methylene phosphonate) and inhibition of $CaCO_3$ crystal growth, Phosphorus, Sulfur Silicon Relat. Elem. 179(3) (2004) 627–648.

[38] Z. Amjad, P.G. Koutsoukos, Evaluation of maleic acid based polymers as scale inhibitors and dispersants for industrial water applications, Desalination 335 (2014) 55–63.

[39] B. Akın, M. Oner, Y. Bayram, K.D. Demadis, Effects of carboxylate-modified, "Green" inulin biopolymers on the crystal growth of calcium oxalate, Cryst. Growth Des. 8 (2008) 1997–2005.